

Conf - 911111 - 20

2  
PNL-SA--19318

DE92 006421

HELIUM GENERATION RATES IN ISOTOPICALLY  
TAILORED Fe-Cr-Ni ALLOYS IRRADIATED IN  
FFTF/MOTA

CONFIDENTIAL  
JAN 21 1992

L. R. Greenwood  
B. M. Oliver

F. A. Garner

November 1991

Presented at the  
5th International Conference on  
Fusion Reactor Materials  
November 17-22, 1991  
Clearwater, Florida

Work supported by  
the U.S. Department of Energy  
under Contract DE-AC06-76RL0 1830

Pacific Northwest Laboratory  
Richland, Washington 99352

**DISCLAIMER**

This report was prepared as an account of work sponsored by an agency of the United States Government. Neither the United States Government nor any agency thereof, nor any of their employees, makes any warranty, express or implied, or assumes any legal liability or responsibility for the accuracy, completeness, or usefulness of any information, apparatus, product, or process disclosed, or represents that its use would not infringe privately owned rights. Reference herein to any specific commercial product, process, or service by trade name, trademark, manufacturer, or otherwise does not necessarily constitute or imply its endorsement, recommendation, or favoring by the United States Government or any agency thereof. The views and opinions of authors expressed herein do not necessarily state or reflect those of the United States Government or any agency thereof.

MASTER

8

# HELIUM GENERATION RATES IN ISOTOPICALLY TAILORED FE-CR-NI ALLOYS IRRADIATED IN FFTF/MOTA

L.R. Greenwood, F.A. Garner, and B.M. Oliver<sup>a</sup>

<sup>1</sup>Pacific Northwest Laboratory, P.O. Box 999, Richland, WA 99352 USA

<sup>a</sup>Rockwell International, Rocketdyne, Division, 6633 Canoga Ave., Canoga Park, CA 91303 USA

## Abstract

Three Fe-Cr-Ni alloys have been doped with 0.4% <sup>59</sup>Ni for side-by-side irradiations of doped and undoped materials in order to determine the effects of fusion-relevant levels of helium production on microstructural development and mechanical properties. The alloys were irradiated in three successive cycles of the Materials Open Test Assembly (MOTA) located in the Fast Flux Test Facility (FFTF). Following irradiation, helium levels were measured by isotope dilution mass spectrometry. The highest level of helium achieved in doped alloys was 172 appm at 9.1 dpa for a helium(appm)-to-dpa ratio of 18.9. The overall pattern of predicted helium generation rates in doped and undoped alloys is in good agreement with the helium measurements.

## Introduction

Fusion reactors will produce significant levels of helium in materials due to  $(n,\alpha)$  reactions with 14 MeV neutrons. In iron-based engineering alloys, helium will be produced at a rate of about 10 appm per atomic displacement (dpa). Concern has been raised that these elevated helium levels could affect the evolution of microstructural damage and thereby affect mechanical properties. Irradiations in fast reactors generally produce helium at levels which are 10% or less than those of fusion levels. Consequently, techniques have been devised to elevate helium production to simulate fusion reactor conditions.

In the present experiment, Fe-Cr-Ni alloys were doped with 0.4% of <sup>59</sup>Ni [1] which has a high  $(n,\alpha)$  cross section for low-energy neutrons. The addition of natural nickel is a well-known technique for elevating helium production in mixed-spectrum reactors due to the  $^{58}\text{Ni}(n,\gamma)^{59}\text{Ni}(n,\alpha)$  sequential reaction[2]. However, unlike the present experiment, time is required for the burn-in of <sup>59</sup>Ni before helium production becomes significant. This delay in helium production in mixed-spectrum reactors may impact the experiment strongly, especially during the incubation phase of microstructural development.

In a recent series of papers on the use of <sup>59</sup>Ni isotopic doping, it has been shown that single-variable comparisons of the effect of helium at fusion-relevant generation rates do not support a significant role for helium in determining the tensile properties of simple austenitic alloys [3-6]. This is in contrast to the results of comparative irradiation studies conducted at significantly different displacement rates [7-9] or at helium generation rates significantly higher than that of anticipated fusion environments[8,9].

---

<sup>1</sup>Pacific Northwest Laboratory is operated for the U.S. Department of Energy by Battelle Memorial Institute under Contract DE-AC06-76RLO 1830.

## Experimental Measurements

Three alloys were prepared for the present irradiations, namely Fe-15Cr-25Ni, Fe-15Cr-25Ni-0.04P, and Fe-15Cr-45Ni. In each case, some of the alloy was doped with 1.98%  $^{59}\text{Ni}$  and some was left undoped using only natural nickel[1]. The  $^{59}\text{Ni}$  content was 1.58% for Fe-15Cr-25Ni and Fe-15Cr-25Ni-0.04P, and 0.88% for Fe-15Cr-45Ni. For the purposes of this study, the small addition of phosphorous is insignificant and shall be ignored. The alloys were then irradiated in three successive experiments in the MOTA position of the FFTF. Samples were originally placed in five different levels of the MOTA-1D subassembly at temperatures between 365-600°C. This experiment lasted for 185.8 EFPD from August 17, 1985, to July 19, 1986, at a power level of 400 MW. After irradiation, these alloys and additional unirradiated alloys were inserted into MOTA-1E from September 10, 1986, to September 10, 1987, attaining 341.8 EFPD at 291 MW. Following this, two sets of alloys were additionally irradiated in MOTA-1F from November 18, 1987, to January 8, 1989, reaching 335.4 EFPD at 291 MW. Irradiations further continued in MOTA-1G; however, these samples were removed from the reactor on March 19, 1991, and their helium levels have not yet been analyzed. Details of these irradiations are discussed further in reference 10.

Following irradiation, samples of the various alloys were analyzed for their helium content at Rockwell International's Rocketdyne Division. The measurements were performed using a specialized gas mass spectrometer system [11]. Each sample was prepared by cutting two "quarter" specimens from each original transmission electron microscope (TEM) disk. The specimens were then acid-etched to remove the outer 0.02 to 0.04 mm of surface to eliminate any corrections for alpha-recoil effects. Final specimen masses ranged from 2 to 3 mg.

Each of the helium analyses involved vaporizing the specimen in a resistance-heated graphite crucible in one of the mass spectrometer systems' high-temperature vacuum furnaces, and then measuring the  $^4\text{He}$  released relative to a known quantity of added  $^3\text{He}$  spike (isotope dilution method). The helium spikes were obtained by expanding and partitioning a known quantity of  $^3\text{He}$  gas through a succession of accurately calibrated volumes [12]. The mass sensitivity was determined by analyzing various combinations of  $^3\text{He}$  and  $^4\text{He}$  spikes. Mass discrimination for  $^3\text{He}$  and  $^4\text{He}$  was typically 1.5. Measured helium values ranged from  $2 \times 10^{12}$  to  $6 \times 10^{15}$  atoms.

The results of the helium measurements, in terms of helium concentration, are summarized in Table 1, which also lists the position in the reactor, dpa, and  $^{59}\text{Ni}$  doping conditions. Conversion from total measured helium to helium concentration was based on the specimen mass and on atom concentration values determined for each alloy ( $\approx 1.07 \times 10^{22}$  atoms/g). The helium concentration values in Table 1 represent average values for the duplicate analyses conducted on each sample. The uncertainty following each value represents the total estimated ( $1\sigma$ ) uncertainty. Average reproducibility between the duplicate helium analyses was 0.9%.

The dpa calculations were performed with the SPECTER computer code[13]. Note that the quoted dpa values are alloy-dependent. For example, in the

below-core basket, the Fe-15Cr-45Ni alloy received 9.1 dpa during cycles 1D and 1E, while the Fe-15Cr-25Ni alloy received only 8.6 dpa. This difference is caused by the higher dpa rate for nickel than iron. Both of these alloys have higher dpa rates than pure iron or stainless steel. The small increase in dpa due to the  $^{59}\text{Ni}(n,\alpha)$  reaction was also included, as discussed later.

### Helium Calculations

The production of helium from  $^{58}\text{Ni}$  is determined by the expression [2]:

$$\frac{N(\text{He})}{N_o(^{58}\text{Ni})} = \frac{\sigma_\alpha [\sigma_T (1 - e^{-\sigma_\gamma \phi t}) - \sigma_\gamma (1 - e^{-\sigma_T \phi t})]}{\sigma_T (\sigma_T - \sigma_\gamma)} \quad (1)$$

where  $N(\text{He})$  = helium atoms produced at time  $t$   
 $N_o(^{58}\text{Ni})$  = initial number of  $^{58}\text{Ni}$  atoms  
 $\sigma_\alpha$  =  $^{59}\text{Ni}(n,\alpha)$  cross section  
 $\sigma_T$  =  $^{59}\text{Ni}$  total absorption cross section  
 $\sigma_\gamma$  =  $^{58}\text{Ni}(n,\gamma)$  cross section  
 $\phi$  = total neutron flux  
 $t$  = irradiation time

This equation applies to all irradiations with nickel, including the undoped alloy, and should be further multiplied by 0.683 to account for the abundance of  $^{58}\text{Ni}$ . However, in fast reactors, the main source of helium is due to threshold  $(n,\alpha)$  reactions with all isotopes of nickel, iron, and chromium. These threshold reactions are assumed to produce helium by a linear product of the cross section times the neutron fluence. Although one usually associates the  $^{58}\text{Ni}(n,\gamma) ^{59}\text{Ni}(n,\alpha)$  two-step reaction with thermal neutrons, the epithermal flux in fast reactors is large enough to produce significant levels of helium.

In the case of  $^{59}\text{Ni}$  doping, equation 1 simplifies, as follows:

$$N(^{59}\text{Ni}) = N_o(^{59}\text{Ni}) e^{-\sigma_T \phi t} \quad (2)$$

$$N(\text{He}) = N_o(^{59}\text{Ni}) \frac{\sigma_\alpha}{\sigma_T} (1 - e^{-\sigma_T \phi t}) \quad (3)$$

The first equation above incorporates the burn-up of  $^{59}\text{Ni}$ , which was as high as 30% in the present irradiations. Neutron cross sections for the  $(n,\alpha)$ ,  $(n,p)$ , and  $(n,\gamma)$  reactions from  $^{59}\text{Ni}$  and for the  $(n,\gamma)$  reaction from  $^{58}\text{Ni}$  were taken from the ENDF/B-V evaluation[14]. The burnup cross section was taken as the sum of the three reaction cross sections for  $^{59}\text{Ni}$ . Previously, we have published data showing that these equations and neutron cross sections give excellent agreement with helium measurements in mixed-spectrum reactors[14]. Displacement damage calculations and helium production from natural nickel, chromium, and iron were provided by the SPECTER computer code.[14] There is also a small increase in displacement damage due to the energetic (340 keV)  $^{56}\text{Fe}$  recoils from the  $^{59}\text{Ni}(n,\alpha)$  reaction (i.e., additional dpa = helium(appm)/567) [2]. This dpa enhancement has been included in the

calculations for both doped and undoped specimens; however, the maximum difference is only 0.2 dpa for any of the irradiated alloys.

In order to adequately calculate helium production for these experiments, it is essential to have measurements of the neutron fluence and energy spectra. Unfortunately, dosimetry data have not been completely analyzed for all of these irradiations. Hence, it was necessary to rely on neutron flux and spectral calculations to fully map the helium production in the MOTA; such calculated neutron spectra were available from cycle 9A [15]. Fluence gradient and neutron spectral dosimetry measurements were performed for selected locations in the MOTA-1E and MOTA-1F experiments [16]. Comparison between the calculations and dosimetry measurements supports the validity of the calculations. Such comparisons show generally good agreement between dosimetry and calculations for in-core positions; however, the dosimetry measurements are consistently higher than calculations for above-core and below-core positions.

Thus it is not expected that the present calculations will give an exact fit to the helium data. Rather, the intent is to show that we can generally describe the data and more importantly predict the behavior of helium generation in doped and undoped alloys throughout the MOTA assembly.

### Helium Production Calculations for FFTF/MOTA

Helium production calculations are illustrated in Figure 1 for Fe-15Cr-45Ni as a function of axial location in the MOTA assembly after completion of the MOTA-1E and MOTA-1F irradiations (677.2 EFPD at 291 MW). The bottom curve shows helium production for the undoped alloy and the top curve includes the enhanced helium from the  $^{59}\text{Ni}$ -doped alloy. There is some additional helium even in the undoped alloy due to burn-in of  $^{59}\text{Ni}$  from  $^{58}\text{Ni}(n,\gamma)$ . The undoped alloy helium production curve is similar in shape to that of the neutron fluence and dpa curves, although there is a slight bulge in the below-core region caused by the burn-in of  $^{59}\text{Ni}$ . The helium production from the  $^{59}\text{Ni}$ -doped alloy more clearly shows the effects of the changing neutron spectrum. Outside the FFTF core region (-45 to +45 cm) there is a rapid increase in epithermal neutrons, resulting in an increase in helium production. The maximum helium production occurs in the below core basket (-70 to -55 cm). The helium production curve is not axially symmetric due to differing distributions of steel supports and sodium coolant.

The peculiar axial dependence of the helium production from  $^{59}\text{Ni}$ -doping enhances the variation of the He(appm)-to-dpa ratio as a function of axial location, as shown in Figure 2. In-core, the He/dpa ratio nearly doubles as a result of the doping. However, the ratio climbs to fusion-like values of 10-19 for out-of-core positions for the doped alloy. Note that the undoped alloy curve also shows a slight increase below core due to the buildup of  $^{59}\text{Ni}$  from  $^{58}\text{Ni}$ .

Figure 3 shows the time dependence of the helium-to-dpa ratio at the midplane of the FFTF/MOTA in both the doped and undoped alloys. The small but steady increase in both ratios is due to the burn-in of  $^{59}\text{Ni}$ , an effect that

is often neglected in computing helium generation in fast reactor experiments. It is also evident from Figure 3 that at midplane much higher  $^{59}\text{Ni}$  doping levels would be needed to significantly increase helium production. Fusion-like He/dpa levels would require  $^{59}\text{Ni}$  doping of 10-15%, which would be difficult to produce or handle. Figure 4 shows the time-dependent helium production in the below-core basket of the MOTA. Because of the higher flux of epithermal neutrons, there is a clear decrease in the helium/dpa ratio for the doped alloy due to burn-up of  $^{59}\text{Ni}$  and a much sharper percentage increase in the ratio for the undoped alloy due to burn-in of  $^{59}\text{Ni}$ .

### Comparison of Helium Measurements and Calculations

Helium measurements and calculations are compared in Table I. These data span four different reactor positions; two different alloys, both doped and undoped; and four different combinations of FFTF reactor cycles. Radial flux gradients were ignored for the present calculations; however, calculations show that the flux varies by about 8% across the MOTA subassembly [15]. We should also note that recent calculations indicate that the presence of various moderating materials or highly neutron absorbing materials in the MOTA can have significant influence (9-15% flux depression) on the neutron energy spectrum in nearby irradiation positions. Nevertheless, for level 1 in-core, level 6 just above core, and the below-core basket, the measurements (M) and calculations (C) agree within 30%. The larger disagreement for level 8 is known to be due to flux uncertainties in the neutron diffusion calculations. Comparison with the available dosimetry data [16,17,18] indeed shows that the calculated flux at -66 cm is low by about 20-30%. This difference is in good agreement with the C/M ratios near 0.75 for the below-core position. Similarly, dosimetry data at +123 cm is about 25-50% higher than calculated for level 8; this would explain the low C/M ratios of 0.34-0.41 found for this position.

Work currently in progress for MOTA-2A includes complete neutron spectral measurements for all levels of the MOTA. Analysis of these data will provide a more complete picture of the uncertainties in the neutron energy spectra; such information will also be applicable to previous MOTA irradiations. Additional helium measurements are also planned for the MOTA-1G irradiation, which was performed concurrently with the MOTA-2A experiment.

### Conclusions

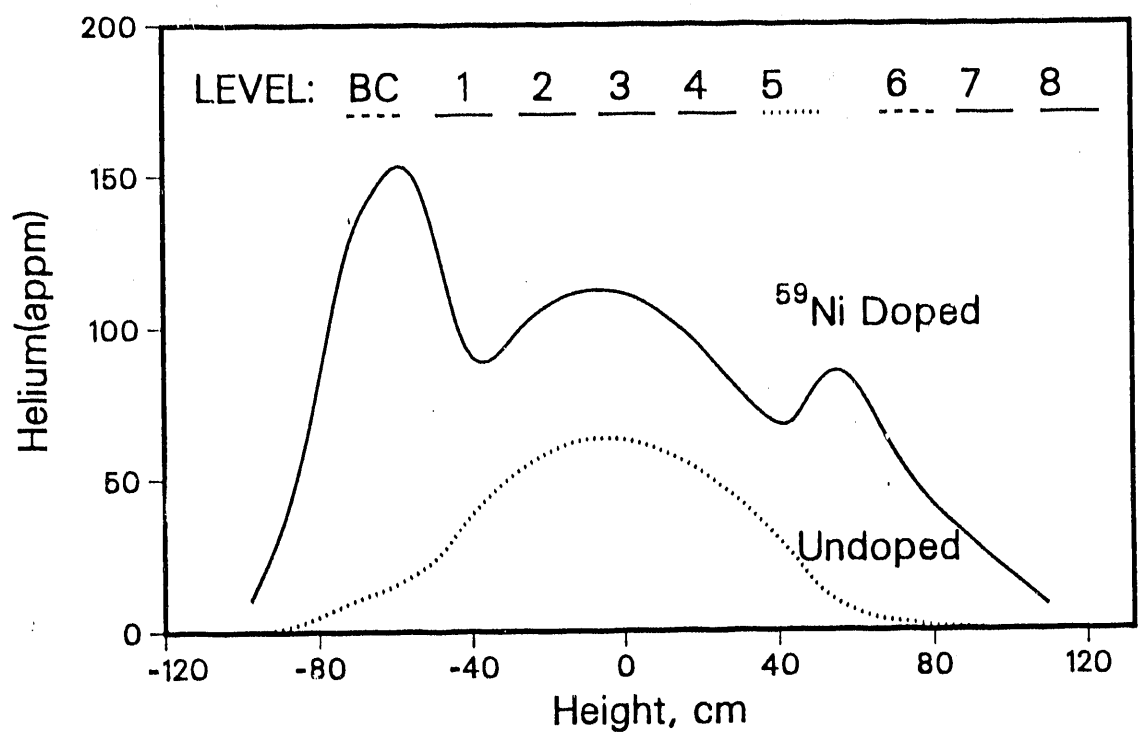
The present calculations, and their agreement with the available helium data, support the model of helium production in both doped and undoped alloys and indicate that helium levels for the in-core irradiation positions can be accurately predicted. However, at present, uncertainties in the neutron energy spectrum limit our ability to predict helium production for out-of-core positions. Consequently, it is essential that accurate helium measurements be performed for these experiments so that we can properly account for helium effects and correlate property changes accordingly. Similarly, neutron dosimetry measurements must be pursued in order to define the energy spectrum in all positions of the MOTA. This will be particularly important for out-of-core positions that are finding increasing use for irradiations of fusion materials.

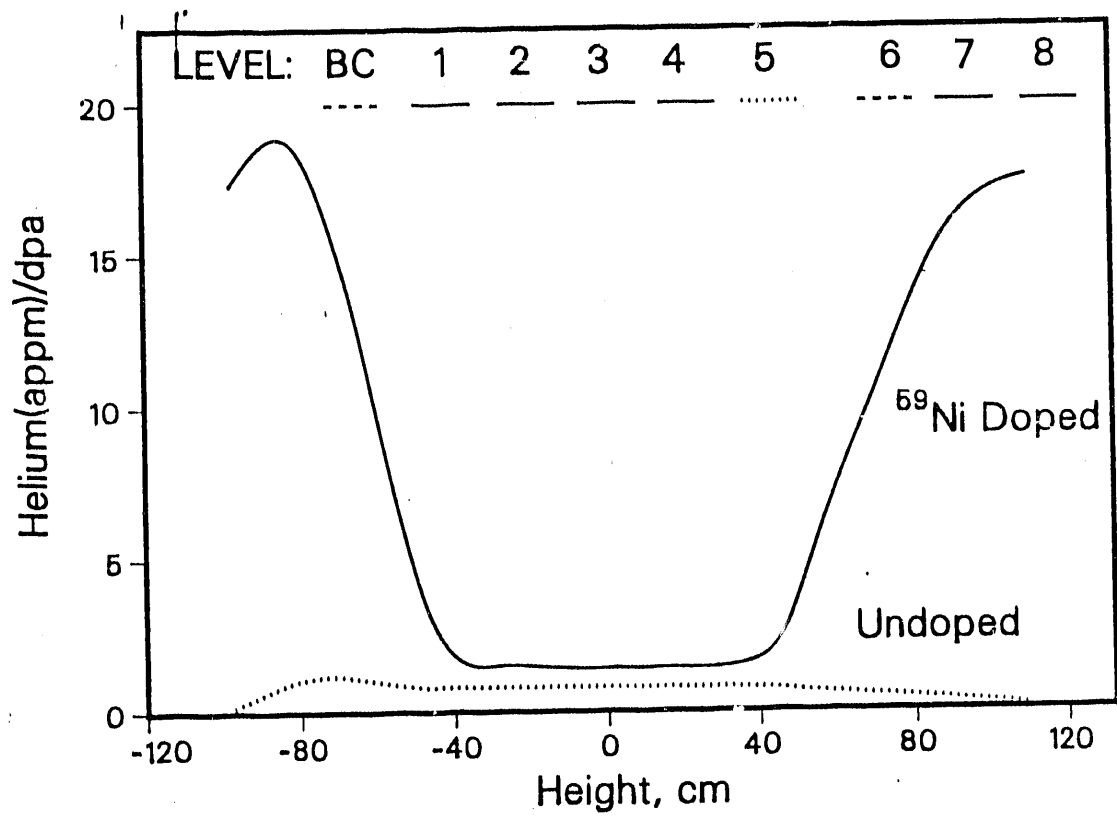
## References

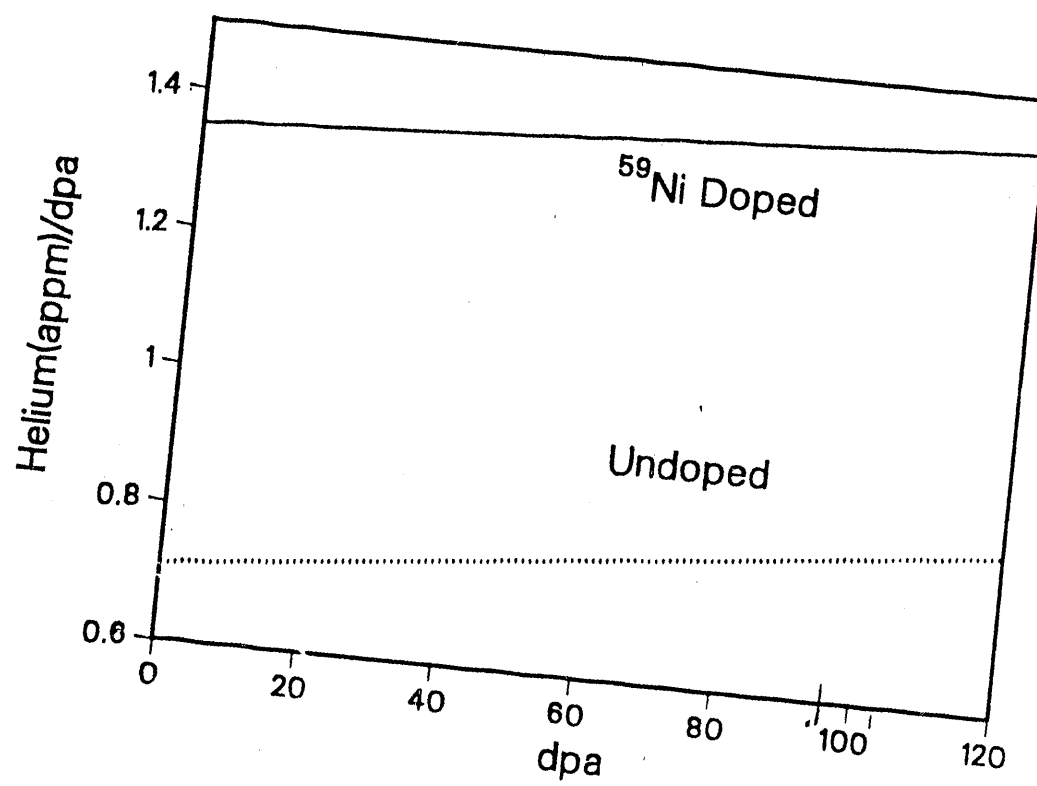
- 1) R.L. Simons, H.R. Brager, and W.Y. Matsumoto, J. Nucl. Mater., 141-143(1986)1057-1060.
- 2) L.R. Greenwood, J. Nucl. Mater., 115(1983)137-142.
- 3) M. L. Hamilton and F. A. Garner, these proceedings.
- 3) F. A. Garner, M. L. Hamilton, R. L. Simon and M. K. Maxon, J. Nucl. Mater., 179-181(1991)554-557.
- 5) J. F. Stubbins and F. A. Garner, J. Nucl. Mater., 179-181(1991)523-525.
- 6) H. Kawanishi, F. A. Garner and R. L. Simons, J. Nucl. Mater., 179-181(1991)511-514.
- 7) A. F. Rowcliffe, A. Hishinuma, M. L. Grossbeck and S. Jitsukawa, J. Nucl. Mater., 179-181(1991)125-129.
- 8) M. L. Hamilton, A. Okada and F. A. Garner, J. Nucl. Mater., 179-181(1991)558-562.
- 9) N. Sekimura, F. A. Garner and R. D. Griffin, these proceedings.
- 10) M.L. Hamilton, F.A. Garner, and B.M. Oliver, Fusion Reactor Materials Semiannual Progress Report, DOE/ER-0313/9(1990)61-68.
- 11) H. Farrar IV and B.M. Oliver, J. Vac. Sci. Technol. A4 (1986) 1740.
- 12) B.M. Oliver, J.G. Bradley, and H. Farrar IV, Geochim. Cosmochim. Acta 48 (1984) 1759.
- 13) L.R. Greenwood and R.K. Smither, ANL-FPP/TM-197 (1985).
- 14) L.R. Greenwood, D.W. Kneff, R.P. Skowronski, and F.M. Mann, J. Nucl. Mater. 122-123(1984)1002-1010.
- 15) R.L. Simons, Westinghouse Hanford Company, private communication (1990).
- 16) L.R. Greenwood, Fusion Reactor Materials Semiannual Progress Report, DOE/ER-0313/9 (1990)31-36.
- 17) R.L. Simons, Damage Analysis and Fundamental Studies Quarterly Progress Report, DOE/ER-0046/21 (1985) 10-14.
- 18) L.S. Kellogg, W.N. McElroy, and W.Y. Matsumoto, private communication (1989).

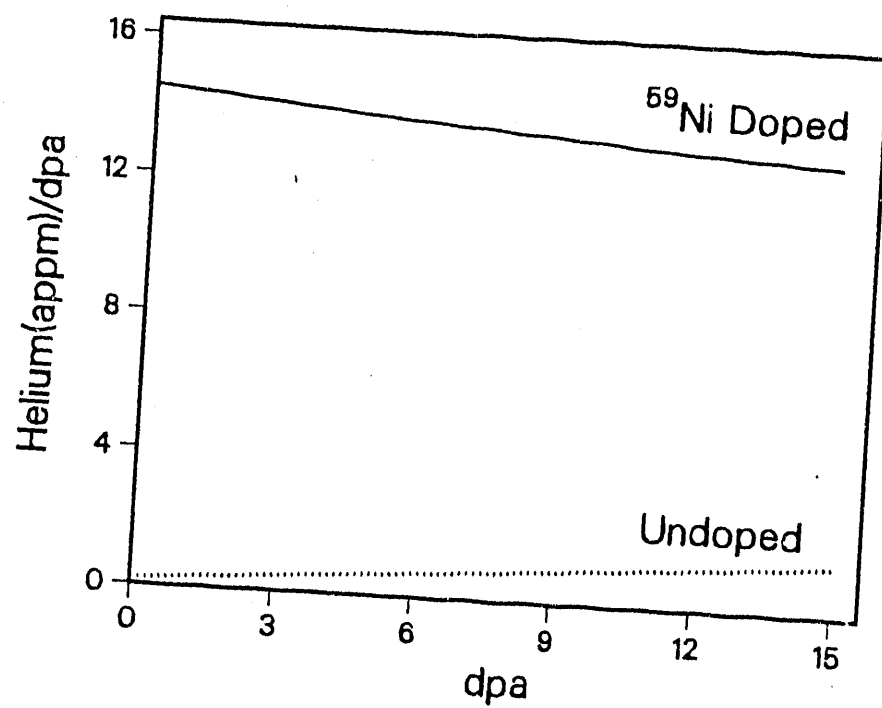
## Figure Captions

- 1) Helium production (appm) for both  $^{59}\text{Ni}$ -doped and undoped Fe-15Cr-45Ni alloy as a function of height in the MOTA assembly after the 1E and 1F irradiation.
- 2) Helium(appm)-to-dpa ratios for both  $^{59}\text{Ni}$ -doped and undoped Fe-15Cr-45Ni alloy as a function of height in the MOTA assembly after the 1E and 1F irradiation.
- 3) Helium/dpa ratio vs. dpa for both  $^{59}\text{Ni}$ -doped and undoped Fe-15Cr-45Ni alloy near midplane (+2.6 cm) of the MOTA assembly.
- 4) Helium/dpa ratio vs. dpa for both  $^{59}\text{Ni}$ -doped and undoped Fe-15Cr-45Ni alloy in the below core basket (-65.9 cm) of the MOTA assembly.









DATE  
FILMED  
2/21/192

I

